Approximation of Force and Energy in Vehicle Crash Using LPV Type Description

ISTVÁN Á. HARMATI
Széchenyi István University
Dept. of Mathematics and Computational Sciences
Egyetem tér 1, 9026 Győr
HUNGARY
harmati@sze.hu

ANDRÁS RÖVID
Óbuda University
John von Neumann Faculty of Informatics
Bécsi út 96/B, 1034 Budapest
HUNGARY
rovid.andras@nik.uni-obuda.hu

PÉTER VÁRLAKI
Budapest University of Technology and Economics
Dept. of Chassis and Lightweight Structures
Bertalan L. u. 1, 1111 Budapest
HUNGARY
varlaki@kme.bme.hu

Abstract: In accident analysis, vehicle crash mechanics and vehicle safety research modeling of the deformational force and absorbed energy plays a crucial role. The usually applied FEM based methods give good approximations, but they have extremely large computational complexity and require a detailed knowledge about the parameteres of the crash and the vehicle. There are simpler models, but they not give satisfactory approximation. In this paper using the LPV-HOSVD paradigm we introduce a model for vehicle deformation process, which well approximates the deformation force and the absorbed energy, moreover it has acceptable computational complexity.

Key–Words: Vehicle crash, force model, LPV model, tensor product transformation, higher order singular value decomposition (HOSVD).

1 Introduction

For all of the car factories one of the most important task is to develop better and better passive and active vehicle safety systems. In most of the cases in the field of vehicle crash mechanics, accident analysis, accident reconstruction and crash analysis the estimation of the energy absorbed by the deformation of the car body is a key issue, it plays important role in precise reconstruction of the whole accident. This project requires a lot of vehicle crash tests and computer simulations, and applying the results of these efforts, different kind of models are developed for passanger safety, vehicle stiffness, etc. So for vehicle engineers one of the most important task is to find an 'as simple as possible' model for the deformational force and the absorbed kinetic energy, which gives acceptable approximation, but doesn't need perfect knowledge about the parameters of the vehicle ([1], [2],[3]).

There are many tools developed to support the accident reconstruction and analysis, but to reconstruct the accident properly, they require accurate input data. The usual way to develop a detailed model of the highly nonlinear deformation processes (not only in the field of vehicle crash) is based on a kind of finite element method (FEM) ([4], [5], [6], [7]). This approach gives a complete description about the whole deformation process, but requires a detailed, accurate knowledge about the geometry of the vehicle and the circumstances, and about the material properties of the vehicle (which are not known exactly in general), and as a consequence of the huge number of freedom, the computer simulation demands extremely large computational power.

But if we are contented with an approach, which not gives such detailed information about the process, but works well in aspect of some important features (for example deformation force and absorbed energy vs. time), a simpler model is more suitable ([1], [3], [8], [9],[10], [11]).

In the followings we introduce a model for vehicle deformation, which well approximates the force and the absorbed energy during the deformational process. This approach gives good approximation and has acceptable computational complexity.

2 Previous Force Models and Real Crash Tests

2.1 Previous Simple Force Models

There are several attempts to find simple force models, which describe the deformational process approximately well, but not require too many knowledge about the parameters of the vehicle, and require enermous computational cost. The most widely used force models are introduced below.

- Linear force model (also known as Campbell model). It was established by K. Campbell, based on the works of Emori [12].

$$F(x) = kx$$

- Bilinear force model (it would be better to cite it as piecewise linear, but in the literature of vehicle crash it known as bilinear force model [13], [14]).

$$F(x) = \begin{cases} k_1 x & \text{if } x \leq x_{bl} \\ k_1 x_{bl} + k_2(x - x_{bl}) & \text{if } x > x_{bl} \end{cases}$$

- Force saturation model ([13], [14], [15]). This is a special case of the bilinear model, when $k_2 = 0$.

$$F(x) = \begin{cases} kx & \text{if } x \leq x_s \\ kx_s & \text{if } x > x_s \end{cases}$$

- Power law force model ([16]). This is the most sophisticated within the introduced models. In the other models the stiffness of a vehicle decreases with the depth of deformation, but not so easy to find a good physical or mechanical interpretation for 'breakpoint' of the force curve. Opposite with this, the power law model gives a smooth transition between linear and saturated parts of the curve, moreover the smoothness makes the further examinations relatively easy.

$$F(x) = k_0 x_N \left(\frac{x}{x_N} \right)^n$$

Easy to see that the main difference between these models is based on the handling of the notion of stiffness. All of the models are certain generalizations of the very simple linear model, and achieve better approximation applying a more and more complex stiffness concept.

2.2 The 'Stiffness' of a Vehicle

The stiffness of a vehicle is a widely used quasi-heuristic notion in the field of crash and accident analysis, accident reconstruction and vehicle safety research ([17], [18], [19], [20]). The stiffness, as a numerical value, is unambiguous in case of the linear model (but vehicle deformation processes usually are not describable effectively using this simple method). There are several approaches defining the notions of stiffness ([21]). From a certain point of view these are generalizations of the stiffness of the linear modell ('k'), and yield stiffness which depends on the depth of the deformation.

- Local stiffness (derivative of the force–deformation curve in a certain point).

$$k_{loc} = \frac{dF}{dx}$$

- Energy equivalent or global stiffness. The stiffness value is the coefficient of a linear model, which belongs to the same absorbed energy (E) and to the same deformation (x).

$$k_{gl} = \frac{2E}{x^2}$$

- Slope of the line fitted to certain part of the force–deformation curve.
- Stiffness from average deformation force:

$$\frac{1}{2} kd^2 = \overline{F} \cdot d \Rightarrow k = \frac{2\overline{F}}{d}$$

- Local maxima (peaks) in the force-deflection curve are also used to describe the stiffness.

2.3 LCB Crash Test Data

In the field of vehicle safety research there are several type of crash tests. For our purpose the most suitable is the so called load cell barrier (LCB) test. Within this approach the examined vehicle is driven into a special barrier which is equipped with force-sensors. During the collision a set of sensors in the back of the car measures acceleration, while force-sensors measure the deformation force at the wall.

We work with data which are available from the free database of NHTSA (National Highway Traffic Safety Administration, USA): *http://www.nhtsa.dot.gov*. We will use data series of three different LCB tests in which a similar type of car was examined with different impact speed.

These data are available 'as measured' form, so we have to filter them before of further computing. There are rigorous prescriptions for filtering the crash test data [22]. According to SAE J211 the force and acceleration data were filtered with CFC60 filter. From the acceleration data the deformation is determined by double integration, so after filtering we have two data sets: force vs. time and deformation vs. time (See Fig. 2). From these one can easily produce the force–deflection curve (See Fig. 3), which can be compared with the force models described above.

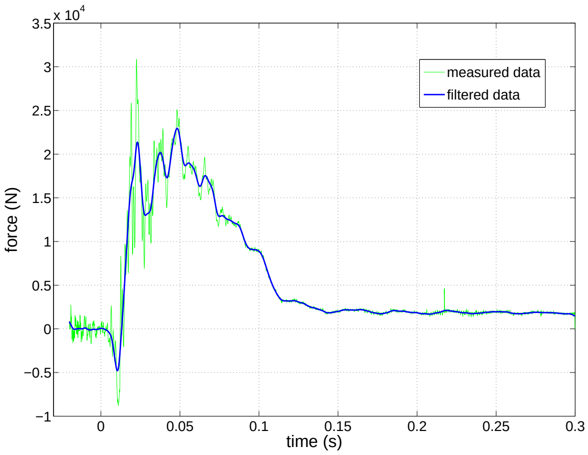

Figure 1: The measured force and the force after filtering by CFC60 filter vs. time.

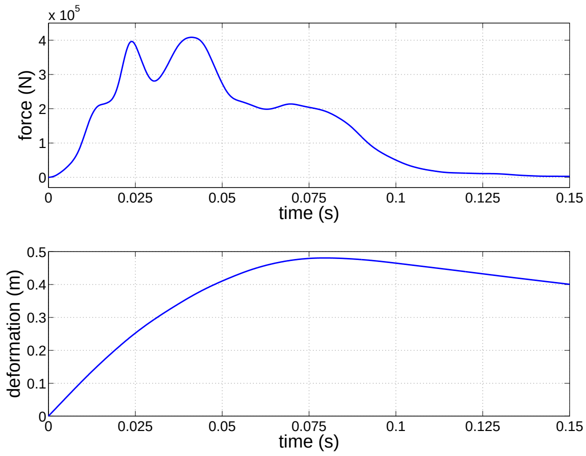

Figure 2: Filtered force and computed deformation vs. time from a real crash test.

We can observe that the first region of the curve is not so far from the linear, but after there appear local maxima and minima, the nonlinearity of the force–deflection relation will be more dominant. Also important to observe the turning back end of the curve: this means that the deformation process has an elastic component (elastic recovery) (see Fig 3, Fig 4).

Analyzing the usual force models we can state that those are too simple to be able to describe the peaks and the elastic recovery in the force–deflection curve. Moreover, from the concepts of stiffness it is clear, that this cannot be the same numerical value during the deformation process for the whole car body. Based on these experiences we are searching for a model, which approximates the measured data more better and which is a kind of generalization of the linear $(k \cdot x)$ model, but deals with a non-constant stiffness.

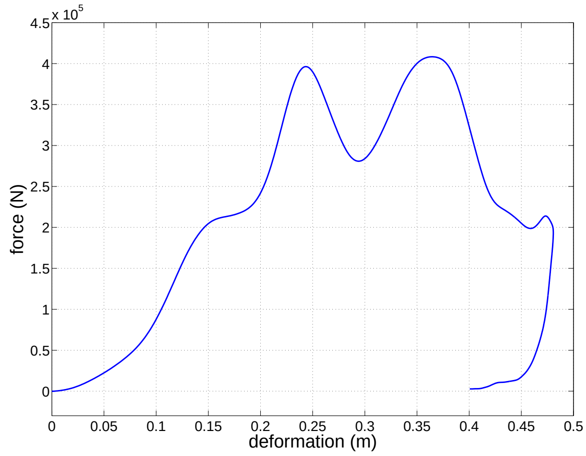

Figure 3: Force-deflection curve derived from the previous force vs. time and deformation vs. time curves.

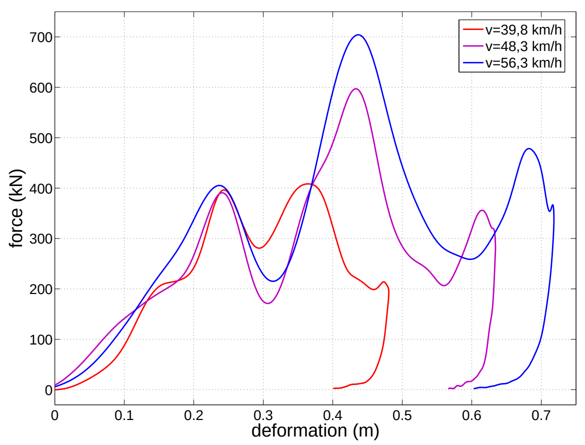

Figure 4: Force-deflection curves for the same type of vehicles at different impact velocities.

3 Mathematical Background of Model Reduction

Singular value decomposition is one of the most powerful tools of linear algebra and it has a great variety of applications. In the last two decade the increasing computing power made it possible to work with large multidimensional arrays (tensors). Some properties of tensors is the same as of matrices in the 'usual' linear algebra, but some of them is a bit trickier (see for example [23], [24]). In this section we shortly introduce the generalization of the singular value decomposition to higher dimesional tensors, and the HOSVD-based model reduction of LPV systems. For more details see for example [25], [26]and [27].

3.1 HOSVD based Canonical form

Consider the following linear parameter varying (LPV) state-space model:

$$\begin{pmatrix}\dot{\mathbf{x}}(t)\\ \mathbf{y}(t)\end{pmatrix} = \mathbf{S}(\mathbf{p}(t))\begin{pmatrix}\mathbf{x}(t)\\ \mathbf{u}(t)\end{pmatrix} \tag{1}$$

where $\mathbf{p}(t) = (p_1(t), ..., p_N(t)) \in \Omega$ and which can be given in the form of

$$\begin{pmatrix}\dot{\mathbf{x}}(t)\\ \mathbf{y}(t)\end{pmatrix} = \left(\mathcal{S} \boxtimes_{n=1}^{N} \mathbf{w}_n^T(p_n)\right)\begin{pmatrix}\mathbf{x}(t)\\ \mathbf{u}(t),\end{pmatrix} \tag{2}$$

where column vector $\mathbf{w}_n(p_n) \in \mathbb{R}^{I_n}$ $n = 1, \ldots, N$ contains one variable bounded and continuous weighting functions $w_{n,i_n}(p_n)$, $(i_n = 1 \ldots I_n)$. The $(N+2)$-dimensional coefficient (system) tensor $\mathcal{S} \in \mathbb{R}^{I_1\times\cdots\times I_{N+2}}$ is constructed from linear time invariant (LTI) vertex systems

$$\mathbf{S}_{i_1\ldots i_N} = \{S_{i_1\ldots i_N,\alpha,\beta}, 1 \leq \alpha \leq I_{N+1}, 1 \leq \beta \leq I_{N+2}\}$$

$$\mathbf{S}_{i_1\ldots i_N} \in \mathbb{R}^{I_{N+1}\times I_{N+2}}.$$

Symbol $\boxtimes_n$ represents the n-mode tensor-matrix product.

For this model, we can assume that the functions $w_{n,i_n}(p_n)$,$i_n = 1, \ldots, I_n$, $n = 1, \ldots, .N$, are linearly independent over the intervals $[a_n, b_n]$, respectively.

The linearly independent functions $w_{n,i_n}(p_n)$ are determinable by the linear combinations of orthonormal functions (for instance by Gram–Schmidt-type orthogonalization method): thus, one can determine such a system of orthonormal functions for all n as $\varphi_{n,i_n}(p_n)$, $1 \leq i_n \leq I_n$, respectively defined over the intervals $[a_n, b_n]$, where all $\varphi_{n,k_j}(p_n)$, $1 \leq j \leq I_n$ are the linear combination of w_{n,i_j}, where i_j is not larger than k_j for all j. The functions w_{n,i_j} can respectively be determined in the same way by functions φ_{n,k_j}. Thus, if the form (2) of (1) exists then we can determine it in equivalent form as follows:

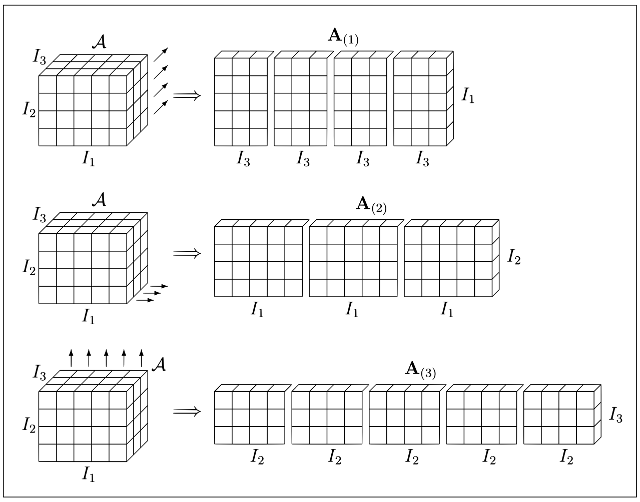

Figure 5: The three possible ways of expansions of a 3-dimensional array into matrices.

$$\begin{pmatrix}\dot{\mathbf{x}}(t)\\ \mathbf{y}(t)\end{pmatrix} = \left(\mathcal{C} \boxtimes_{n=1}^{N} \varphi_n^T(p_n(t))\right)\begin{pmatrix}\mathbf{x}(t)\\ \mathbf{u}(t)\end{pmatrix}, \tag{3}$$

where tensor $\mathcal{C}$ has constant elements, and column vectors $\varphi_n(p_n(t))$ consists of elements $\varphi_{n,k_n}(p_n(t))$.

Corollary 1 *We can assume, without the loss of generality, that the functions w_{n,i_n} in the tensor-product representation of $\mathbf{S}(\mathbf{p})$ are given in orthonormal system:*

$$\forall n : \int_{a_n}^{b_n} w_{n,i}(p_n)w_{n,j}(p_n)dp_n = \delta_{i,j}, \quad 1 \leq i,j \leq I_n,$$

where $\delta_{i,j}$ is the Kronecker-function ($\delta_{ij} = 1$, if $i = j$ and $\delta_{ij} = 0$, if $i \neq j$).

Theorem 2 (HOSVD) *(see Fig 5 and Fig 6) Every tensor $\mathcal{S} \in \mathbb{R}^{I_1\times\cdots\times I_L}$ can be written as the product*

$$\mathcal{S} = \mathcal{D} \boxtimes_{l=1}^{L} \mathbf{U}_l \tag{4}$$

in which

1. $\mathbf{U}_l = \begin{bmatrix}\mathbf{u}_{1,l} & \mathbf{u}_{2,l} & \ldots & \mathbf{u}_{I_l,l}\end{bmatrix}$ *is an orthogonal $(I_l \times I_l)$-matrix called l-mode singular matrix.*

2. *tensor $\mathcal{D} \in \mathbb{R}^{I_1\times\ldots\times I_L}$ whose subtensors $\mathcal{D}_{i_l=\alpha}$ have the properties of*

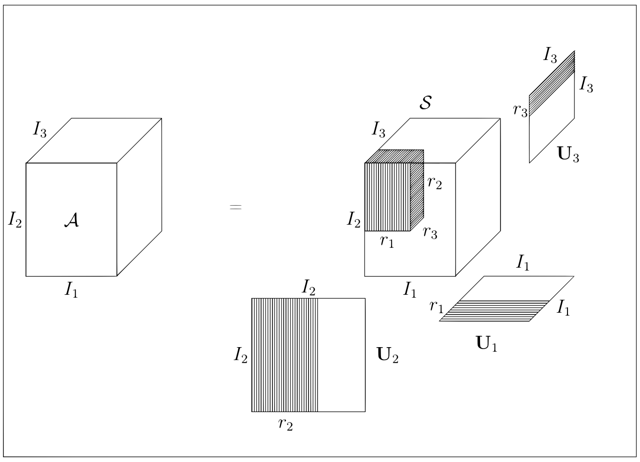

Figure 6: Illustration of the higher order singular value decomposition for a 3-dimensional array. Here S is the core tensor, the U_l-s are the l-mode singular matrices.

(a) *all-orthogonality: two subtensors $\mathcal{D}_{i_l=\alpha}$ and $\mathcal{D}_{i_l=\beta}$ are orthogonal for all possible values of l, α and β : $\langle \mathcal{D}_{i_l=\alpha}, \mathcal{D}_{i_l=\beta} \rangle = 0$ when $\alpha \neq \beta$,*

(b) *ordering: $\|\mathcal{D}_{i_l=1}\| \geq \|\mathcal{D}_{i_l=2}\| \geq \cdots \geq \|\mathcal{D}_{i_l=I_l}\| \geq 0$ for all possible values of l.*

3. *The Frobenius-norm $\|\mathcal{D}_{i_l=i}\|$, symbolized by $\sigma_i^{(l)}$, are l-mode singular values of $\mathcal{D}$ and the vector $\mathbf{u}_{i,l}$ is an i-th singular vector. $\mathcal{D}$ is termed core tensor.*

Theorem 3 (Compact HOSVD) *For every tensor $\mathcal{S} \in \mathbb{R}^{I_1 \times \cdots \times I_L}$ the HOSVD is computed via executing SVD on each dimension of $\mathcal{S}$. If we discard the zero singular values and the related singular vectors $\mathbf{u}_{r_l+1}, \ldots, \mathbf{u}_{I_l}$, where $r_l = rank_l(\mathcal{S})$, during the SVD computation of each dimension then we obtain Compact HOSVD as:*

$$\mathcal{S} = \widetilde{\mathcal{D}} \boxtimes_{l=1}^{L} \tilde{\mathbf{U}}_l, \tag{5}$$

which has all the properties as in the previous theorem except the size of $\mathbf{U}_l$ and $\mathcal{D}$. Here $\tilde{\mathbf{U}}_l$ has the size of $I_l \times r_l$ and $\widetilde{\mathcal{D}}$ has the size of $r_1 \times \ldots \times r_L$.

Consider (1) which has the form of (2). Then we can determine:

$$\begin{pmatrix} \dot{\mathbf{x}}(t) \\ \mathbf{y}(t) \end{pmatrix} = \left(\mathcal{D}_0 \boxtimes_{n=1}^{N} \mathbf{w}_n(p_n(t)) \right) \begin{pmatrix} \mathbf{x}(t) \\ \mathbf{u}(t) \end{pmatrix}, \tag{6}$$

via executing CHOSVD on the first N-dimension of $\mathcal{S}$. The resulting tensor $\mathcal{D}_0 = \tilde{\mathcal{D}} \boxtimes_{n=N+1}^{N+2} \tilde{\mathbf{U}}_n$ has the size of $r_1 \times \ldots \times r_N \times I_{N+1} \times I_{N+2}$, and the matrices $\tilde{\mathbf{U}}_k \in \mathbb{R}^{I_k \times r_k}$, $k = N+1, N+2$ are orthogonal.

The weighting functions have the property of:

1. The r_n number of weighting functions $w_{n,i_n}(p_n)$ contained in vector $\mathbf{w}_n(p_n)$ form an orthonormal system.
2. The weighting function $\mathbf{w}_{i,n}(p_n)$ is an i-th singular function on dimension $n = 1..N$.

Tensor $\mathcal{D}$ has the properties as:

1. Tensor $\mathcal{D} \in \mathbb{R}^{r_1 \times \ldots \times r_{N+2}}$ whose subtensors $\mathcal{D}_{i_n=i}$ have the properties of
   (a) all-orthogonality: two subtensors $\mathcal{D}_{i_n=i}$ and $\mathcal{D}_{i_n=j}$ are orthogonal for all possible values of n, i and j : $\langle \mathcal{D}_{i_n=i}, \mathcal{D}_{i_n=j} \rangle = 0$ when $i \neq j$,
   (b) ordering: $\|\mathcal{D}_{i_n=1}\| \geq \|\mathcal{D}_{i_n=2}\| \geq \ldots \geq \|\mathcal{D}_{i_n=r_n}\| > 0$ for all possible values of $n = 1, \ldots, N+2$.
2. The Frobenius-norm $\|\mathcal{D}_{i_n=i}\|$, symbolized by $\sigma_i^{(n)}$, are n-mode singular values of $\mathcal{D}$.
3. $\mathcal{D}$ is termed core tensor consisting the LTI systems.

3.2 Tensor Product Transformation

Tensor product (TP) transformation is numerical approach, which make a connection between linear parameter varying models and higher order tensors ([25], [27], [28]). The main steps are the followings:

- Discretize the LPV model over a hyper-rectangular grid in the parameter space (dimension is defined by the number of the parameters). If we deal with state space representation, we get matrices $\mathbf{S}^{D}_{m_1 m_2 \ldots m_N}$.
- Store the matrices into the tensor $\mathcal{S}^D \in \mathbb{R}^{M_1 \times M_2 \times \ldots M_N \times O \times I}$.
- Execute HOSVD on the first N dimension of tensor $\mathcal{S}^D$ and we get the following:

$$\mathcal{S}^D \approx \mathcal{S} \bigotimes_{n=1}^{N} \mathbf{U}_n$$

  Tensor $\mathcal{S} \in \mathbb{R}^{I_1 \times I_2 \times \cdots \times I_N \times O \times I}$ contains the LTI (parameter independent) matrices.
- The weighting functions for the LTI matrices are stored in discretized form in the columns of matrices $\mathbf{U}_n$.

4 LPV Type Force Model

The results of crash tests show difficult force and displacement behaviors. From this, it is obvious that the stiffness parameter of a vehicle (or a part of the vehicle) is not a constant value, but depends on several variables. From practical point of view we search for a model, where the stiffness depends on the measure of deformation (x) and on the impact velocity of the vehicle (v).

4.1 The Structure of the Model

Based on the fact mentioned above, we assume the force can be approximated well by a nonlinear form, which is a generalization of the linear spring model:

$$F = k(x, v)x. \tag{7}$$

Or, in differential equation form:

$$m\ddot{x} = k(x, v)x. \tag{8}$$

From this, with $k' = k(x, v)/m$, $x_1 = x$ and $x_2 = \dot{x}_1$ we obtain the following matrix form:

$$\begin{pmatrix} \dot{x}_1 \\ \dot{x}_2 \end{pmatrix} = \begin{pmatrix} 0 & 1 \\ k' & 0 \end{pmatrix} \begin{pmatrix} x_1 \\ x_2 \end{pmatrix}. \tag{9}$$

This is a parameter varying matrix and our main assumption is that the behavior of original system (force and displacement) can be described quite well using this kind of nonlinearity. In general state-space model form

$$\begin{aligned} \dot{\mathbf{x}}(t) &= f(\mathbf{x}(t)) \\ y(t) &= c(\mathbf{x}(t)) \end{aligned} \tag{10}$$

where

$$\begin{aligned} f(\mathbf{x}(t)) &= \begin{pmatrix} x_2(t) \\ k\left(x_1(t), v\right) \end{pmatrix} \\ c(\mathbf{x}(t)) &= \begin{pmatrix} x_1(t) & 0 \end{pmatrix} \end{aligned} \tag{11}$$

With the usual notation of LPV models:

$$\begin{pmatrix} \dot{\mathbf{x}}(t) \\ y(t) \end{pmatrix} = \mathbf{S}(\mathbf{p}(t)) \begin{pmatrix} \mathbf{x}(t) \\ u(t) \end{pmatrix}. \tag{12}$$

The system matrix $\mathbf{S}(\mathbf{p}(t))$:

$$\mathbf{S}(\mathbf{p}(t)) = \begin{pmatrix} \mathbf{A}(\mathbf{p}(t)) & \mathbf{B}(\mathbf{p}(t)) \\ \mathbf{C}(\mathbf{p}(t)) & \mathbf{D}(\mathbf{p}(t)) \end{pmatrix}. \tag{13}$$

where $\mathbf{p}(t) = (x_1(t), v)$ and

$$\mathbf{A} = \begin{pmatrix} 0 & 1 \\ k' & 0 \end{pmatrix}, \quad \mathbf{B} = \begin{pmatrix} 0 \\ 0 \end{pmatrix}, \tag{14}$$

$$\mathbf{C} = \begin{pmatrix} 1 & 0 \end{pmatrix}, \quad \mathbf{D} = \begin{pmatrix} 0 \end{pmatrix}.$$

4.2 Identification of Parameter k'

The next task is to determine the function k'. The approach is similar to the methods introduced in [29] and [30]. Firstly the functional dependence of k' on the variables x (depth of deformation) and v (impact speed) must be specified, for example piecewise linear, polynomial, spline or other linear combinations of given functions of x and v.

The model identification includes two major steps: identification of the local models (LTI models) with the same structure of the LPV model and on the base of these models identification of the final LPV model.

4.2.1 Identification of the Local Models

For local model identification we need some data from well-measured crash tests: depth of deformation vs. time, force (at sensors) vs. time. From this data set for a certain deformation x a linear spring model can be identified. Certainly, for other x an other model is valid. The stiffnes k' depends on x, x depends on time (t), so we handle k' as a function of t, which is determined by the measured $F(t)$ and $x(t)$. In this way, for a certain impact speed a set of simple linear models is determined. After that we have to repeat this measuring and identifying process at other impact speeds, but with the same division on the parameter t. Finally we get a large amount of local models in the space of the impact velocity (v) and the time (t), with the same structure of the searched LPV.

4.2.2 Identification of the Final LPV Model

A set of linear models means a set of certain values of the parameter varying k' at different parameter values. From these points and using our assumption about the type of the functional dependence, the function k' identified.

4.3 Reduction of the LPV Model

Because of the large amount of obtained parameter independent models our system may become very complex. In order to reduce the complexity of the system we apply tensor product transformation and higher order singular value decomposition, which were introduced within the mathematical tools. As we will see, for an acceptable approximation of the deformational force and absorbed energy we do not have to keep all of the singular values, but only a few of them.

5 Application of the Model on Real Crash Test Data

The method described above was executed on real crash tests data taken from NHTSA. There were three different impact velocity, deformation in time and force in time were measured. From these data sets we obtained by interpolation the functions $F(t, v)$ and the $x(t, v)$, which determined the $k(t, v)$ stiffness (see Fig 7, Fig 8 and Fig 9).

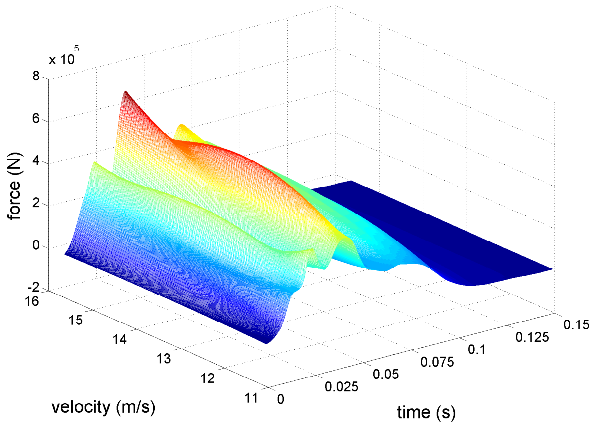

Figure 7: The interpolated surface of the force vs. impact velocity and time ($F(v, t)$).

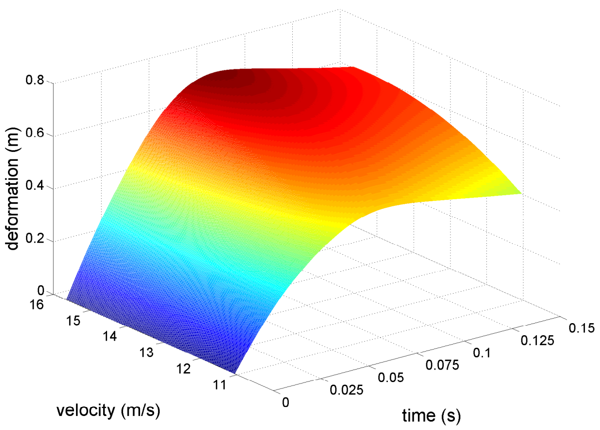

Figure 8: The interpolated surface of the deformation vs. impact velocity and time ($x(v, t)$).

5.1 HOSVD Based Reduction

The computation was carried out with Matlab TPToolbox ([28]). We applied 108 grid lines in the dimension of the time and 34 grid lines in the dimension of the velocity. Computing HOSVD on each dimension we

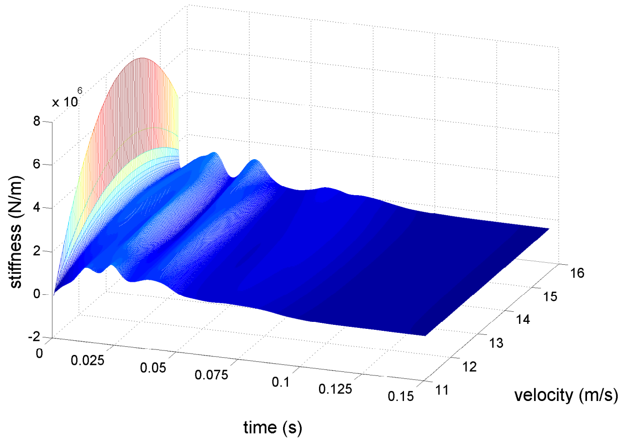

Figure 9: The surface of the stiffness vs. impact velocity and time, obtained form the force and the deformation surfaces ($k'(v, t)$).

got 10-10 singular values (which are numerically not zero). So the maximal model was given by keeping all of these singular values. Neglecting singular values step by step we can check the approximation capability of the reduced models (see Fig. 10, 11 and 12).

5.1.1 Approximation Capability of the Reduced Model in Case of Deformation Force

As we can see, if we keep three singular values the reduced model produces practically the measured data. If we keep less singular values the approximation becames worse, but the main features of the curve appears in these cases also. The approximation is better in case of the medium velocity (see Table 1).

Table 1: Mean square errors of the deformation force (n: number of remaining singular values).

n	Velocity (km/h)		
	39.8	48.3	56.3
1	5.1399	0.7598	6.0068
2	0.0148	0.4926	6.3828
3	0.0045	0.0178	0.0456
4	0.0043	0.0178	0.0447
5	0.0044	0.0179	0.0449

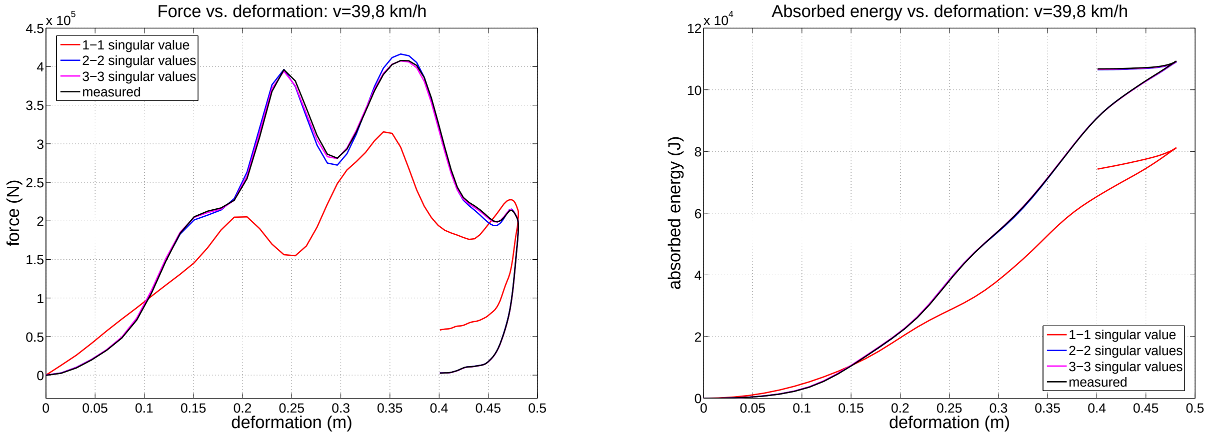

Figure 10: Comparison of the measured data and the reduced models (impact velocity: 39.8 km/h).

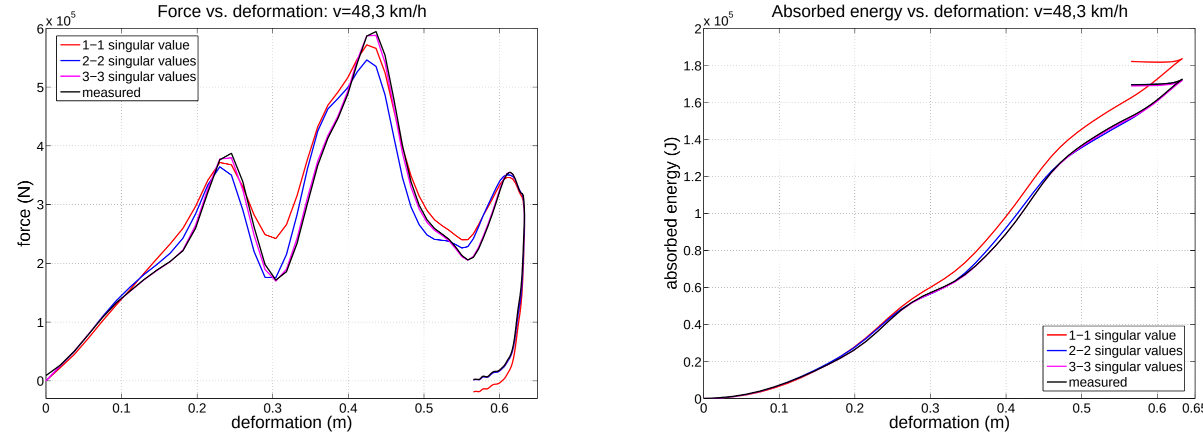

Figure 11: Comparison of the measured data and the reduced models (impact velocity: 48.3 km/h).

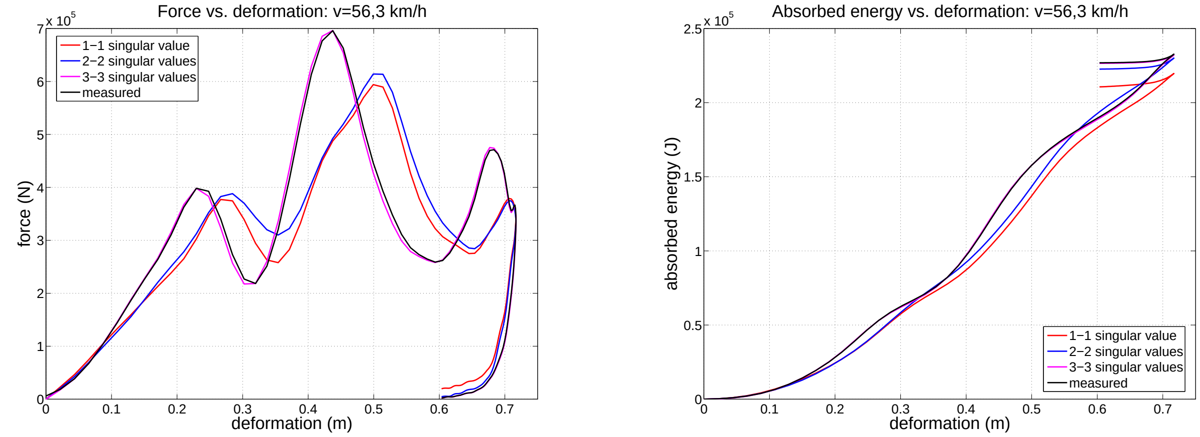

Figure 12: Comparison of the measured data and the reduced models (impact velocity: 56.3 km/h).

5.1.2 Approximation Capability of the Reduced Model in Case of Absorbed Energy

Before analyzing the results of the reduced models we have to examine the notion of absorbed energy. During the deformation process the kinetic energy of the vehicle turns to deformation energy. It is easy to determine the absorbed energy from the force-deflection curve: the absorbed energy is the area under the curve. As it can be seen from the force-deflection curve, the mechanical deformation has two major part: residual and elastic deformation. From this it is clear that not the whole kinetic energy of the vehicle turns to residual deformation (the area of the 'loop'), but a little part of it became kinetic energy again (the area under the final part of the force curve), while the damaged vehicle pushes back (elastic recovery). For this reason the maximal absorbed energy is not equal to the residual absorbed energy, and this results the 'flag' at the end of the absorbed energy vs. deformation curve.

As in the case of the force, the reduced model with only three singular values is the same as the measured data. But if we keep only two singular values the result is almost the same (see Table 2). So for good approxmation of the absorbed energy we need less singular values than for good approximation of the force.

Table 2: Mean square errors of the estimated absorbed energy (n: number of remaining singular values).

n	Velocity (km/h)		
	39.8	48.3	56.3
1	6.3929	0.9908	1.6565
2	0.0004	0.0079	0.2466
3	0.0002	0.0033	0.0023
4	0.0002	0.0033	0.0026
5	0.0002	0.0033	0.0024

6 Conclusion

Applying the LPV-HOSVD paradigm we introduced a method based on real crash test data for modeling the force and the absorbed energy during the vehicle deformational process. This model based on the natural fact that the stiffness of a vehicle depends on the depth of deformation and on the impact velocity. The applied concept of the stiffness is more complex than the stiffness notions used in the field of vehicle crash mechanics and accident analysis, but the model gives more better approximation, and with the HOSVD based reduction the complexity of the model can be reduced significantly, while the approximation capability remains satisfactory.

Acknowledgements: The research was sponsored by OTKA CNK 78168 project and Széchenyi István University. A. Rövid was supported by the János Bolyai Research Scholarship of the Hungarian Academy of Sciences.

References:

[1] R.M. Brach, R.M. Brach, *Vehicle accident analysis and reconstruction methods*, SAE International, 2005.

[2] H. Steffan, Accident reconstruction methods, *Vehicle System Dynamics*, Vol. 47, No. 8, 2009, pp. 1049–1073.

[3] M. Huang, *Vehicle Crash Mechanics*, CRC, 2002.

[4] R. Blumhardt, FEM-crash simulation and optimisation, *International Journal of Vehicle Design*, Vol. 26, No. 4, 2001, pp. 331–347.

[5] L. Wågström, R. Thomson, B. Pipkorn, Structural adaptivity in frontal collisions: implications on crash pulse characteristics, *International Journal of Crashworthiness*, Vol. 10, No. 4, 2005, pp. 371–378.

[6] S.W. Kirkpatrick, J.W. Simons, J.W., T.H. Antoun, Development and validation of high fidelity vehicle crash simulation models, *International Journal of Crashworthiness*, Vol. 4, No. 4, 1999, pp. 395–406.

[7] F. Teixeira–Dias, V. Miranda, C. Gameiro, J. Pinho–Da–Cruz, J. Cirne, Impact behaviour of aluminium foam and cork in energy absorption systems, in *Proc. of the WSEAS Int. Conf. on Applied and Theoretical Mechanics*, Venice, Italy, November 22–24, 2006, pp. 148–153.

[8] H.G. Mooi, J. Huibers, Simple and effective lumped mass models for determining kinetics and dynamics of car-to-car crashes, *International Journal of Crashworthiness*, Vol. 5, No. 1, 2000, pp. 7–24.

[9] Z. Moumni, F. Axisa, Simplified modelling of vehicle frontal crashworthiness using a modal approach, *International Journal of Crashworthiness*, Vol. 9, No. 3, 2004, pp. 285–297.

[10] I. Vazquez-Alvarez, J. J. Ocampo–Hidalgo, C. Aviles–Cruz, A. Ferreyra Ramirez, Vehicle mathematical model reduction considering the brake system dynamics, *WSEAS Transactions on Systems*, No. 2, Vol. 9, 2010, pp. 156–166.

[11] J. Zhou, H. Peng, J. Lu, Collision model for vehicle motion prediction after light impact, *Vehicle System Dynamics*, Vol. 46, 2008, pp. 3–15.

[12] R.I. Emori, Scale models of automobile collisions with breakaway obstacles, *Experimental Mechanics*, 13(2), 1973, pp.64–69.

[13] M.S. Varat and S.E. Husher, Vehicle crash severity assessment in lateral pole impacts, *SAE Transactions*, 108(6), 1999, pp.302–324.

[14] C.E. Strother, R.L.Woolley, M.B. James, and C.Y.Warner, Crush energy in accident reconstruction, *SAE Transactions*, (2), 1986, pp.740–756.

[15] K.J. Welsh and D.E. Struble, Crush energy and structural characterization, *SAE Transactions*, Vol. 108, No. 6, 1999, pp.290-301.

[16] R.L. Wooley, Non-linear analysis in accident reconstruction, in *Accident reconstructions (ed. R.M. Brach)*, SAE, 2001.

[17] J.A. Neptune and J.E. Flynn, A Method for Determining Crush Stiffness Coeffcients from Offset Frontal and Side Crash Tests, *SAE Transactions*, 107, 1999, pp.93–109.

[18] J.A. Neptune and J.E. Flynn, A method for determining accident specific crush stiffness coefficients, *SAE Transactions*, 103(6), 1994, pp.1249–1265.

[19] J.F. Kerkhoff, S.E. Husher, M.S. Varat, A.M. Busenga, and K. Hamilton, An Investigation Into Vehicle Frontal Impact Stiffness, BEV and Repeated Testing for Reconstruction, *SAE Spec. Publ.*, SAE, Warrendale, 1993, pp. 227–255.

[20] G.A. Nystrom, G. Kost, and S.M. Werner, Stiffness parameters for vehicle collision analysis, *SAE Transactions*, 100(6), 1991, pp.169–176.

[21] G.S. Nusholtz, Lan Xu, Y. Shi, and L. Di Domenico, Vehicle mass and stiffness: Search for a relationship, *SAE Transactions*, Vol. 113, No. 6, 2004, pp.748-754.

[22] D. Cichos, D. de Vogel, M. Otto, O. Schaar, and S. Zölsch, *Crash Analysis Criteria Description*, Workgroup Data Processing Vehicle Safety, 2006.

[23] L. De Lathauwer, B. De Moor, and J. Vandewalle, A Multilinear Singular Value Decomposition, *SIAM Journal on Matrix Analysis and Applications*, 21(4), 2000, pp. 1253–1278.

[24] N. E. Mastorakis, The singular value decomposition (SVD) in tensors (multidimensional arrays) as an optimization problem. Solution via genetic algorithms and method of Nelder–Mead, *WSEAS Transactions on Systems*, No. 1, Vol. 6, 2007, pp. 17–23.

[25] P. Baranyi, P. Várlaki, and L. Szeidl, Definition of the HOSVD based canonical form of polytopic dynamic models, *IEEE International Conference on Mechatronics*, 2006, pp. 660–665.

[26] P. Baranyi, P. L. Várkonyi, Exact tensor product distributed compensation based stabilization of the TORA system, in *Proc. of the WSEAS Int. Conf. on Dynamical Systems and Control*, Venice, Italy, November 2–4, 2005, pp. 38–43.

[27] L. Szeidl, P. Baranyi, Z. Petres, and P. Várlaki, Numerical Reconstruction of the HOSVD Based Canonical Form of Polytopic Dynamic Models, *Proc. of the International Symposium on Computational Intelligence and Intelligent Informatics*, ISCIII'07, 2007, pp. 111–116.

[28] S. Nagy, Z. Petres, and P. Baranyi, TP Tool-a MATLAB Toolbox for TP Model Transformation, *Proc. of 8th International Symposium of Hungarian Researchers on Computational Intelligence and Informatics*, Budapest, Hungary, 2007, pp. 483–495.

[29] G. Belforte, F. Dabbene, and P. Gay, LPV approximation of distributed parameter systems in environmental modelling, *Environmental Modelling and Software*, 20(8), 2005, pp.1063–1070.

[30] D. Coca and S.A. Billings, Identification of finite dimensional models of infinite dimensional dynamical systems, *Automatica*, 38(11), 2002, pp.1851–1865.